

# Synthesis and Characterization of Indium-Doped ZnO Nanowires with Periodical Single–Twin Structures

Liang Xu,\* Yong Su, Yiqing Chen, Haihua Xiao, Li-ang Zhu, Qingtao Zhou, and Sen Li

School of Materials Science and Engineering, Hefei University of Technology, Hefei, Anhui, 23009 P.R. China

Received: December 23, 2005; In Final Form: February 16, 2006

In-doped ZnO (IZO) nanowires have been synthesized by a thermal evaporation method. The morphology and microstructure of the IZO nanowires have been extensively investigated using scanning electron microscopy (SEM), X-ray diffraction (XRD), and high-resolution transmission electron microscopy (HRTEM). The products in general contain several kinds of nanowires. In this work, a remarkable type of IZO zigzag nanowire with a periodical twinning structure has been investigated by transmission electron microscopy (TEM). HRTEM observation reveals that this type of IZO nanowire has an uncommonly observed zinc blend crystal structure. These nanowires, with a diameter about 100 nm, grow along the [111] direction with a well-defined twinning relationship and a well-coherent lattice across the boundary. In addition, an IZO nanodendrite structure was also observed in our work. A growth model based on the vapor–liquid–solid mechanism is proposed for interpreting the growth of zigzag nanowires in our work. Due to the heavy doping of In, the emission peak in photoluminescence spectra has red-shifted as well as broadened seriously.

## Introduction

Zinc oxide (ZnO) is one of the most promising materials for the fabrication of optoelectronic devices operating in the blue and ultraviolet (UV) region, owing to a direct wide band gap (3.37 eV) and a large exciton binding energy (60 meV).<sup>1,2</sup> Moreover, due to its superior conducting properties based on oxygen vacancies, ZnO has been investigated as a transparent conducting and piezoelectric material for fabricating solar cells, electrodes, and sensors.<sup>3–5</sup> Therefore, one of the most challenging issues in ZnO-related research is to enhance the electrical conductivity and optical properties of ZnO. As is well-known, doping in semiconductors with selective elements offers an effective method to adjust their electrical, optical, and magnetic properties, which is crucial for their practical application. Although masses of research were done on nanostructure doping, it still remains a challenge to achieve efficient carrier density in one-dimension semiconductors.<sup>6,7</sup> Up to now, considerable effort has been focus on the doping of ZnO nanowires. The typical dopants that have been used to enhance the conductivities of ZnO are the group III (B, Al, In, Ga) and group IV (Pb, Sn) elements of the periodic table. In particular, the In-doped ZnO films show similar electrical conductivity and better transparency in both the visible and the infrared regions as compared to indium–tin–oxide (ITO), so they can be widely used as transparent conductors in many applications.<sup>8,9</sup> Indium is selected as the dopant for ZnO nanowires in our work because it is recognized as one of the most efficient elements used to improve the optoelectrical properties of ZnO.<sup>10</sup>

Herein, we report that IZO nanowires have been synthesized with zinc acetate and indium oxide ( $\text{In}_2\text{O}_3$ ) by the thermal evaporation method. Structural investigations reveal that a fraction of IZO nanowires in the as-synthesized samples display a marvelous periodic twinning structure. Crystals with face-centered cubic (fcc) structure frequently show well-defined

twinning as lately observed in a number of metallic nanocrystals. For instance, twins<sup>11–13</sup> have been observed in gold, silicon, and, especially, silver nanowires, in which the 5-fold twinning<sup>14</sup> has been analyzed and modeled in detail. As a significant defect structure, twin boundaries could generate positive energy and are expected to have important effects on electronic and mechanical properties.<sup>15</sup> Mechanical studies indicate that twin boundaries act commonly as dislocation obstacles to affect the deformation behavior as observed in copper nanomaterials.<sup>16</sup> In this paper, we will focus on the investigation of the periodic zigzag twinning structure of IZO nanowires by TEM. This type of IZO nanowire with a zinc blend structure grows along the [111] direction with a well-defined twinning relationship and a well-coherent lattice across the boundary, and the twin boundaries appear regularly with an average periodicity of 100 nm. The zigzag angle between two twinning nanounits is about  $141^\circ$  (i.e. twice the renowned (111) twinning angle of  $70.5^\circ$  for the fcc structure). This novel structure observed in IZO nanowire is expected to have novel properties which enable it to achieve a quantum confinement of carries and excitons and to have potential application in nano-optoelectronics or thermoelectricity.

## Experimental Section

Zn acetate (purity, >99%) and  $\text{In}_2\text{O}_3$  (purity, >99%) powders were mixed with a molar ratio of 10:1 and then pressed into small pills under 10 MPa pressure. The pills were calcined at 500 °C for 5 h and sintered at 900 °C for 12 h in air. After being heat treated, the pills were grinded into powder again and mixed with graphite in a molar ratio of 2:1 and then put in an alumina boat and inserted into a horizontal tube furnace as an evaporation source. Several pieces of  $\text{SiO}_2$ (100 nm)/Si(100) plate coated with 2 nm Au were used as substrates, which were located at downstream positions of source materials. Finally, the entire assembly was heated to 900 °C within 2 h and maintained at this temperature for 30 min. The temperature of the substrates was approximately 700–900 °C during the growth. Ar was used as carrier gas and flowed constantly at a

\* Corresponding author. E-mail: andyxul@163.com. Telephone: +86-551-2901365. Fax: +86-551-2901362.

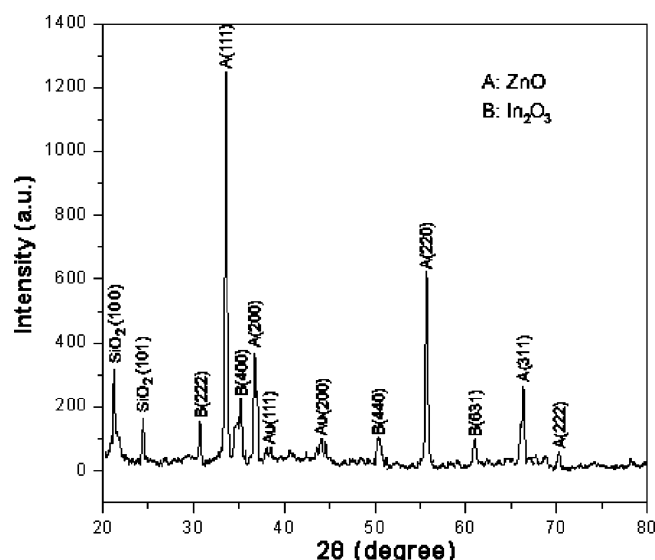


**Figure 1.** XRD pattern of as-synthesized product. The  $\text{SiO}_2$  peaks come from the substrate. A smaller diffraction angle implies a lattice dilatation of the In-doped sample.

rate of 50 standard cubic centimeters/minute (sccm). The chamber pressure was kept at 200 Torr during the experimental process. After the furnace slowly cooled to room temperature, substrates were taken out from the furnace tube. A white product was found on the Au-coated area of the substrates.

The morphologies and structures of the as-deposited products were characterized and analyzed by field-emission scanning electron microscopy (FE-SEM) (JEOL model JSM-6700F), X-ray diffraction (XRD) (MAC Science, model MXPAHF), high-resolution transmission electron microscopy (HRTEM) (JEOL model 2010, operating at 200 kV), and selected area electron diffraction (SAED). Their components were measured via energy-dispersive X-ray spectroscopy (EDS) attached in the

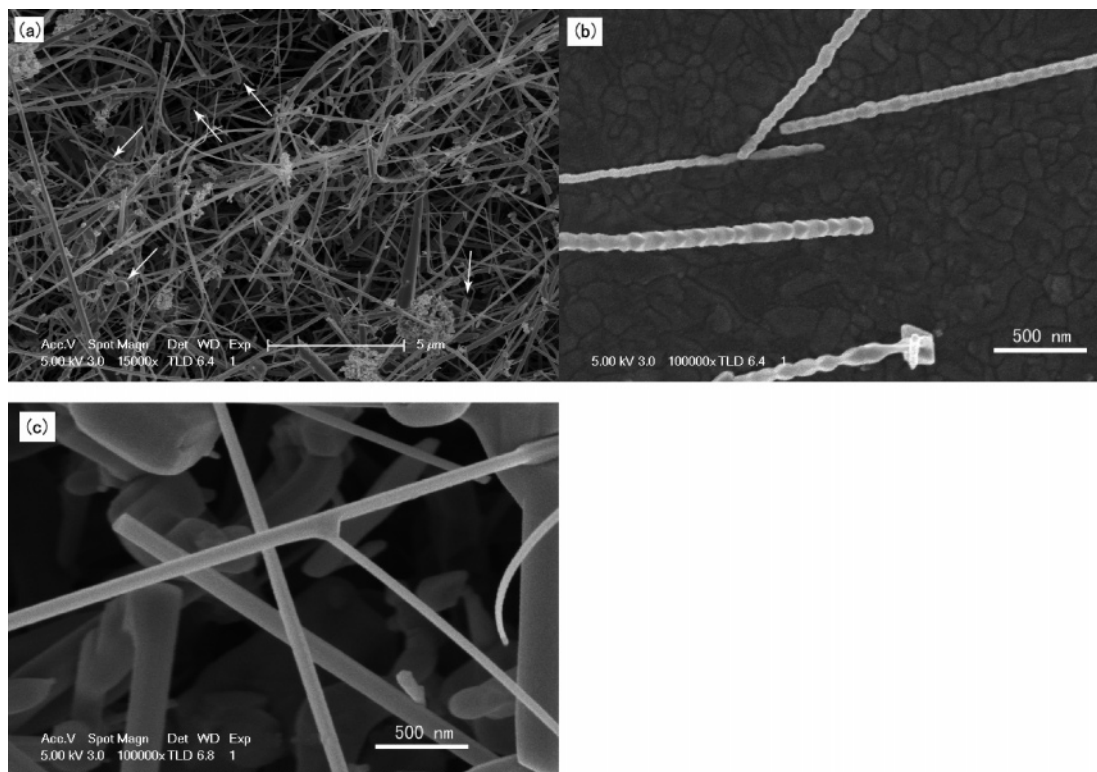
HRTEM system. A photoluminescence (PL) spectrum was measured using a He–Cd laser (260 nm) as the excitation source at room temperature.

## Results and Discussion

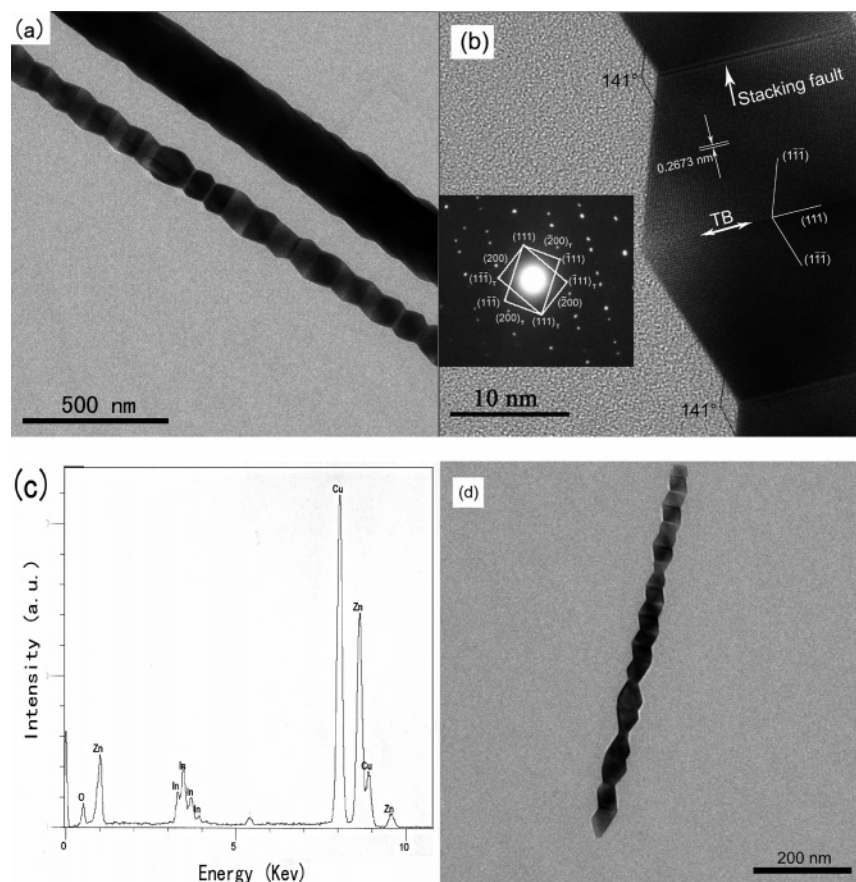
The XRD pattern of the as-synthesized sample is shown in Figure 1. Most of the main diffraction peaks in the XRD spectrum can be indexed to a face-centered cubic zinc blend-structured ZnO with lattice constants of  $a = 4.629 \text{ \AA}$ , which is consistent with the standard values of bulk ZnO (JCPDS 65-2880). Except for the Au and  $\text{SiO}_2$  peaks from the substrate, some peaks corresponding to the residual  $\text{In}_2\text{O}_3$  also exist in this spectrum, revealing a small fraction of  $\text{In}_2\text{O}_3$  also synthesized during the experiment. The intensity of the ZnO(111) peak is much stronger than other ZnO peaks, suggesting the (111) crystal face might be the primary face of the nanowires. This can be further confirmed using HRTEM and the corresponding SAED.

Figure 2a shows a representative FE-SEM of the as-grown products deposited on the Au-coated Si substrates. It illustrates that the products consist of a large quantity of wirelike nanostructure with evidently different geometrical shapes. These nanowires in general have diameters ranging from 20 to 200 nm and lengths of about tens to several hundred micrometers. Catalyst particles shown by some white arrowheads can be observed in the ends of nanowires, indicating a VLS growth process of the nanowires. A typical high-magnification FE-SEM image (Figure 2b) of several nanowires reveals that their geometrical shape is remarkable wavelike and their diameter is about 100 nm. On the other hand, high-magnification FE-SEM observations (Figure 2c) also indicate that a large fraction of the nanowires in the as-grown products display dendritic-crystal morphologies.

To obtain more detail about the structures and compositions of the two types of nanostructures in our product, HRTEM,



**Figure 2.** (a) FE-SEM images of the as-synthesized IZO nanowires with different shapes. (b) High-magnification FE-SEM image of the wavelike nanowires. (c) High-magnification FE-SEM image of the nanowires with dendritic-crystal structures.



**Figure 3.** (a) Typical TEM image of the IZO twinning nanowires displaying a remarkable periodic structure. (b) Corresponding HRTEM image of the local part of the IZO nanowire, clearly showing the twinning turns. (The SAED pattern is shown in the inset, revealing the well-defined (111) twinning relationship in the IZO nanowire.) (c) EDS spectra of the IZO nanowire with periodic single-twinning structure. (d) Another TEM image of a zigzag IZO twinning nanowire with a diameter-modulate structure.

SAED, and EDS measurements were performed to characterize the nanowires. HRTEM observations indicate that most of the product is In-doped ZnO (IZO) nanowires and single-nano-twinning configurations exist in a fraction of the IZO nanowires (20–40%) with diameters ranging from 80 to 120 nm. A representative TEM image of the IZO nanowires shown in Figure 3a reveals that this kind of IZO nanowire has a marvelous periodic zigzag-crystal structure. It is found that the zigzag shapes in the nanowires have nonuniform periodicities. The periodicity of this zigzag structure ranges from 20 to 120 nm as revealed in our TEM observations. These results are different from previous research,<sup>17</sup> in which the periodicities of zigzag shapes in different In/Zn–O layers were almost equal. These differences might be due to the relative low growth temperature of the nanowires (700–900 °C) as compared to that in the solid-state reaction method (>1200 °C).<sup>17</sup> It is expected that long times and high temperature annealing produce an orderly periodic structure in the nanowires.

From the HRTEM image (Figure 3b), we have found that the IZO nanowire has a diameter about 100 nm, and each subunit of the zigzag crystal has a parallelogram shape. The SAED pattern shown as the inset in Figure 3b arises unambiguously from the (111) twinning structure commonly appearing in the face-centered cubic structure systems. All diffraction spots in the present pattern can be easily indexed by twinned nanocrystals. The turning points in general coincide with the twin boundaries and yield a series of parallelogram-shaped nanounits. Figure 3b presents the HRTEM images showing the morphologic properties of twin boundaries (TB), demonstrating the well-defined twinning relationship and the well-coherent lattice cross

the boundary. It is well-known that the {111} twinning angle between two adjacent twin variants in equilibrium is 70.53°;<sup>18</sup> therefore, the zigzag angles as indicated by the broken lines can be given as 141°, in good agreement with the theoretical estimation. In this image, it can be also seen that the nanotwin and stacking fault coexist in the (111) plane and that the spacing between adjacent lattice planes is 0.2673 nm, corresponding to the distance between two (111) planes, which indicates that [111] is the growth direction for the zigzag IZO nanowire. Meanwhile, EDS measurement is also performed to detect the composition of the nanowire (see Figure 3c), which gives a close value of the molar ratio Zn:In  $\approx$  20:1. Moreover, a zigzag diameter-modulate structure is also observed in some regions of the nanowire with a diameter about 50 nm (see Figure 3d). We suggest that the disturbance of the vapor concentration is a major factor that changes the diameter of the catalyst alloy droplets and the growth velocity of nanowires and ultimately results in the diameter-modulated feature in some regions of the zigzag nanowire.

According to the classical explanation, the catalyst particles at the tip of the zigzag nanowires shown both in FE-SEM and in TEM detection are considered as evidence for the operation of the vapor–liquid–solid (VLS) mechanism. For interpreting the experimental result, a possible growth process of the zigzag nanowires is proposed: Zn acetate, In<sub>2</sub>O<sub>3</sub>, and graphite mixed powders were vaporized at elevated temperature, and then the vapors were carried by Ar flow and transported to the position of the substrate. Zn and In vapor reacted with Au and formed little alloy droplets, and solid ZnO precipitated from the droplets in the form of nanowires when ZnO reached the supersaturating



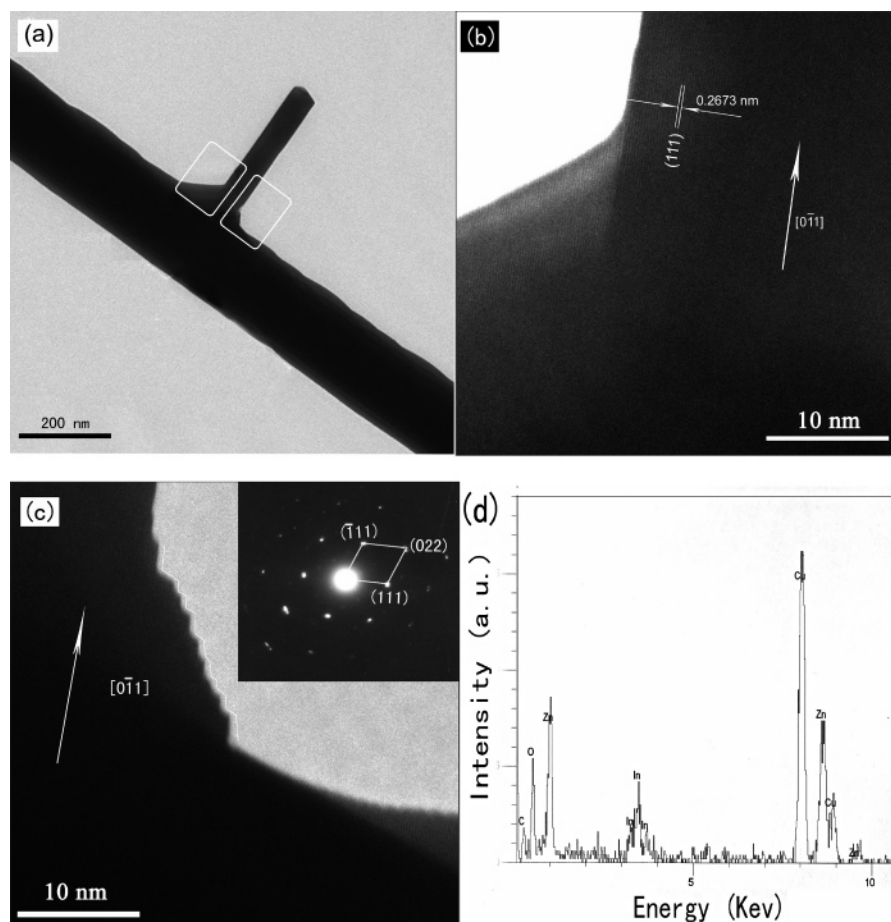


**Figure 4.** (a) Typical TEM image of the nanowires with dendritic-crystal structures. (The two rectangles indicate the region enlarged in the HRTEM images.) (b, c) Corresponding HRTEM images of the left- and right-hand regions of the nanodendrite joint, respectively. (d) EDS spectra of the stem IZO nanowire with a dendritic-crystal structure.

state. At the same time, indium doping was achieved through the process of In substitute Zn atom in ZnO. Continuous feeding of Zn and In atoms into the liquid droplet sustains the growth of the In-doped ZnO nanowires. The frequent and regular appearance of twins directly suggests that the (111) twins are energetically favorable in this kind of nanomaterial. The zigzag structure presented in Figure 3a,b results from the periodic appearance of twin boundaries; therefore, the growth of the zigzag nanowires is driven by the alternative appearance of the twinning variants, as illustrated in the SAED pattern. This indicates that the twin boundary plays as nucleation seeds at the initial growth of the zigzag IZO nanowires.

The IZO nanodendrites is also studied by TEM (see Figure 4a). HRTEM and SAED (Figure 4b,c) results confirm that the dendritic nanowire is single crystalline and that the spacing between adjacent lattice planes is 0.2673 nm, corresponding to the distance between the (111) planes, which indicates that [011] is the growth direction for the ZnO nanowire. Further observation reveals the fringes are continuous in the region of joint, demonstrating that the dendritic nanowire has a uniform structure with diameter about 60 nm. EDS analysis (Figure 4d) reveals that the stem nanowire has a Zn:In atomic ratio of 30:1. Another interesting phenomenon observed in the image (see Figure 4c) is the presence of a contour of steps in the joint region, as schematically marked by a white dashed line. In this region, rows of atoms are missing along [011] and the surface can be qualitatively described to be an irregular "saw-tooth" structure. This atom rearrangement is known as surface reconstruction. As a result of broken bonds, atoms on the surfaces tend to locate at new positions that may be different from the

sites determined by the symmetry of the crystal; thus, a new unit cell is defined to describe the surface structure. Extensive research has been carried out on the surface reconstruction of nanocrystal surfaces, and the most typical<sup>19</sup> example is the reconstruction of the Au{110} surface. From the image (Figure 4c), we can observe that if a row of atoms is missing along [011], the (011) surface transforms into strips of {111} facets. From the energy point of view, it is known that the {111} surface is the most densely packed surface for fcc structure and is thus the most stable surface; the {011} surface is less stable than the {111} surface. Surface reconstruction readily occurs on these surfaces, leading to further reduction of the energy of these surfaces and the formation of the more stable reconstructed surfaces.

As for the formation of the nanodendrites, the dendrite-crystal epitaxial growth mechanism is likely reasonable to explain it. Some temperature fluctuations maybe exist in the vapor around the source material. As a result, once a sporadic prominence occurs on the initial nanofibers, the growth of epitaxial elongation toward the colder vapor starts under a temperature grade, which are the secondary branches. The angle between the secondary and stem branches is related to the relation between their preferential direction.

Two types of IZO nanowires with different morphologies and structures were formed at the same time, which might be attributed to the variety of microcosmic growth conditions. With respect to the unique morphology of the IZO nanowires, it can be concluded that the ratio of In in the reactant has a large effect on the morphology of IZO nanowires. Without In or the small amount of In in the reactants, periodic zigzag nanowires with

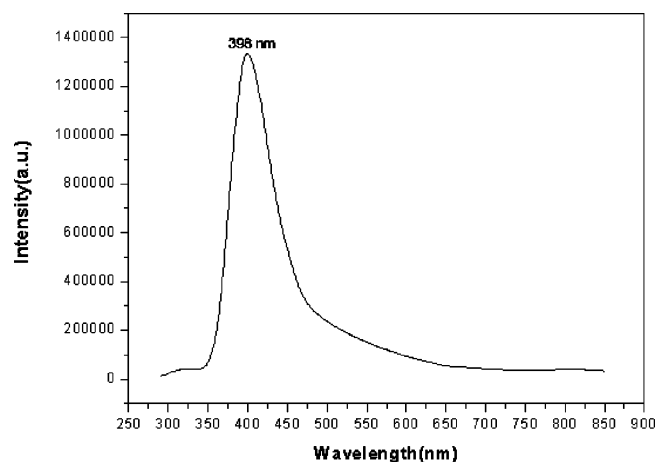


**Figure 5.** PL spectra of the IZO nanowires measured at room temperature.

single-twinning structure cannot be obtained. However, the exact reasons for formation of these subtle periodic structures are yet not clear.

For wide band gap semiconductors, doping in them often induces dramatic changes in their electrical and optical properties<sup>20,21</sup> and markedly alters the band gap ( $E_g$ ). According to the theory of semiconductor-metal transition,  $E_g$  increases when the impurity is kept under Mott critical density,<sup>22</sup> and an abrupt  $E_g$  decrease transition happens while more impurity is doped into the semiconductor. Therefore, heavy doping usually induces an evidently narrowing of  $E_g$ . As well-known, photoluminescence (PL) is a sensitive technique for measuring the band structure of a semiconductor. Figure 5 shows the room-temperature photoluminescence spectra recorded from the as-prepared In-doped ZnO nanowires. There are obvious differences between the PL spectra of doped and undoped ZnO nanowires. Before doping, a sharp UV emission peak at 370 nm (3.351 eV) due to a neutral-donor-bound exciton complex associated with defect pairs ( $D_0$ , X) emissions<sup>23–25</sup> has a small full-width at half-maximum (fwhm) (<1 nm). After doping with indium, the ( $D_0$ , X) emission yields a very weak band near 370 nm, but a new emission band centering at 398 nm (3.115 eV) dominate in the PL spectra. In combination with the structure and component results, the new 398 nm band could be attributed to the emission of heavily In-doped ZnO nanowires and broadened seriously as well as red-shifted strongly to lower energy compared with the emission of undoped ZnO nanowires. The broadening of the emission peak can be interpreted by the formation of band tailing in the band gap, which often is induced by the introduction of an impurity into the semiconductor. The red-shift of UV emission peak should be due to the narrowing of  $E_g$ , which is determined by the carrier concentration in the semiconductor.<sup>26</sup> Kim<sup>27</sup> measured the Mott critical density for In-doped ZnO films and got the result of  $5 \times 10^{19} \text{ cm}^{-3}$ . In our case, the emission peak red-shifted from 3.351 to 3.115 eV, so the  $E_g$  narrowing approximately equals to 240 meV. According to the values given by ref 27, we can estimate the carrier concentration in the heavily doped ZnO nanowires should be as high as  $7 \times 10^{19} \text{ cm}^{-3}$ .

For the undoped ZnO nanowires, there is a visible emission band with center near 490 nm, which has been suggested mainly due to the present of various point defects, either extrinsic<sup>28</sup> or intrinsic.<sup>29</sup> However the center of visible emission band cannot be observed after doping. It is possibly attributed to the existence of In impurities in ZnO nanowires.

## Conclusion

IZO nanowires with periodic single-twinning and homoepitaxial nanodendritic structures have been successfully synthesized by evaporating Zn acetate,  $\text{In}_2\text{O}_3$ , and graphite mixed powders. The morphology and microstructure of this remarkable type of zigzag IZO nanowires have been extensively investigated by HRTEM and EDS, which demonstrated that the IZO nanowires shows an uncommonly observed zinc blend structure. This type of IZO nanowire, with a diameter about 100 nm, grows along the [111] direction with well-defined twinning relationship and the well-coherent lattice across the boundary. The formation mechanism is proposed for interpreting the growth of the zigzag and dendritic-crystal IZO nanowires, respectively. Microstructure characterization indicates that the regular occurrence of single-twinning structure induced the formation of the zigzag IZO nanowires. Furthermore, the PL emission peak has red-shifted as well as broadened seriously because of the heavy doping of In. It should be emphasized that the presence of a regular twinning structure might induce certain specific physical properties in this nanomaterial that are desirable in forthcoming technologic applications. To fabricate nanostructures in a controlled way is a challenge for the development of nanoscience and nanotechnology. We showed that a periodic nanotwinning growth on a nanowire could be realized in the ZnO– $\text{In}_2\text{O}_3$  system. This opens a brand new field to not only nanomaterials synthesis but also their applications in numerous fields.

**Acknowledgment.** This work was financially supported by the National Natural Science Foundation of China (NSFC, Grant No. 20471019) and by the Nature Science Foundation of Anhui province of China (Grant No. 050440904).

## References and Notes

- (1) Cao, H.; Xu, J. Y.; Zhang, D. Z.; Chang, S.-H.; Ho, S. T.; Seelig, E. W.; Liu, X.; Chang, R. P. H. *Phys. Rev. Lett.* **2000**, *84*, 5584.
- (2) Saito, N.; Haneda, H.; Sekiguchi, T.; Ohashi, N.; Sakaguchi, I.; Koumoto, K. *Adv. Mater.* **2002**, *14*, 418.
- (3) Contreras, M. A.; Egaas, B.; Ramanathan, K.; Hiltner, J.; Swartzlander, A.; Hasoon, F.; Noufi, R. *Prog. Photovoltaics* **1999**, *7*, 311.
- (4) Rau, U.; Schmidt, N. *Thin Solid Films* **2001**, *387*, 141.
- (5) Dong, L. F.; Cui, Z. L.; Zhang, Z. K. *Nanostruct. Mater.* **1997**, *8*, 815.
- (6) Seo, H. W.; Bae, S. Y.; Park, J. *Appl. Phys. Lett.* **2003**, *82*, 3752.
- (7) Qi, H.; Wang, C.; Liu, J. *Adv. Mater.* **2003**, *15*, 411.
- (8) Gómez, H.; Maldonado, A.; Asomoza, R.; Zironi, E. P.; Canetas-Ortega, J.; Palacios-Gómez, J. *Thin Solid Films* **1997**, *293*, 117.
- (9) Wang, A.; Dai, J.; Cheng, J.; Chudzik, M. P.; Marks, T. J.; Chang, R. P. H.; Kannewurf, C. R. *Appl. Phys. Lett.* **1998**, *73*, 327.
- (10) Tokumoto, M. S.; Smith, A.; Santilli, C. V.; Pulcinelli, S. H.; Elkaim, E.; Briois, V. *J. Non-Cryst. Solids* **2000**, *273*, 302.
- (11) Lisiecki, I.; Filankembo, A.; Sack-Kongehl, H.; Weiss, K.; Pileni, M.-P.; Urban, J. *Phys. Rev. B* **2000**, *61*, 4968.
- (12) Wang, J.; Tian, M.; Mallouk, T. E.; Chan, M. H. W. *J. Phys. Chem. B* **2004**, *108*, 841.
- (13) Wang, Y. Q.; Smirani, R.; Ross, G. G. *Nano Lett.* **2004**, *4*, 2041.
- (14) Chen, H. Y.; Gao, Y.; Zhang, H. R.; Liu, L. B.; Yu, H. C.; Tian, H. F.; Xie, S. S.; Li, J. Q. *J. Phys. Chem. B* **2004**, *108*, 12038.
- (15) Bietsch, A.; Michel, B. *Appl. Phys. Lett.* **2002**, *80*, 3346.
- (16) Youngdahl, C. J.; Weertman, J. R.; Hugo, R. C.; Kung, H. H. *Scr. Mater.* **2001**, *44*, 1475.
- (17) Li, C.; Bando, Y.; Nakamura, M.; Onoda, M.; Kimizuka, N. *J. Solid State Chem.* **1998**, *139*, 347.
- (18) Shechtman, D.; Feldman, A.; Vaudin, M. D.; Hutchison, J. L. *Appl. Phys. Lett.* **1993**, *62*, 487.
- (19) Wang, Z. L.; Gao, R. P.; Nikoobakht, B.; El-Sayed, M. A. *J. Phys. Chem. B* **2000**, *104*, 5417.
- (20) Sernelius, B. E.; Berggren, K.-F.; Jin, Z.-C.; Hamberg, I.; Granqvist, C. G. *Phys. Rev. B* **1988**, *37*, 10244.
- (21) Sanon, G.; Rup, R.; Mansingh, A. *Phys. Rev. B* **1991**, *44*, 5672.
- (22) Mott, N. F. *Metal–Insulator Transitions*; Taylor and Francis: London, 1974.

- (23) Reynolds, D. C.; Look, D. C.; Jogai, B.; Litton, C. W.; Collins, T. C.; Harsch, W. C.; Cantwell, G. *Phys. Rev. B* **1998**, *57*, 12151.
- (24) Sherriff, R. E.; Reynolds, D. C.; Look, D. C.; Jogai, B.; Hoeisher, J. E.; Collins, T. C.; Cantwell, G.; Harsch, W. C. *J. Appl. Phys.* **2000**, *88*, 3454.
- (25) Matsumoto, T.; Kato, H.; Miyamoto, K.; Sano, M.; Zhukov, E. A.; Yao, T. *Appl. Phys. Lett.* **2002**, *81*, 1231.
- (26) Roth, A. P.; Webb, J. B.; Williams, D. F. *Phys. Rev. B* **1982**, *25*, 7836.
- (27) Kim, K. J.; Park, Y. R. *Appl. Phys. Lett.* **2001**, *78*, 475.
- (28) Dingle, R. *Phys. Rev. Lett.* **1969**, *23*, 579.
- (29) Vanheusden, K.; Seager, C. H.; Warren, W. L.; Tallant, D. R.; Voigt, J. A. *Appl. Phys. Lett.* **1996**, *68*.